

Article

Pseudo-Yang-Lee Edge Singularity Critical Behavior in a Non-Hermitian Ising Model

Liang-Jun Zhai ¹, Guang-Yao Huang ² and Huai-Yu Wang ^{3,*}

¹ The School of Mathematics and Physics, Jiangsu University of Technology, Changzhou 213001, China; zhailiangjun@jsut.edu.cn

² Institute for Quantum Information & State Key Laboratory of High Performance Computing, College of Computer, National University of Defense Technology, Changsha 410073, China; guangyaohuang@quanta.org.cn

³ Department of Physics, Tsinghua University, Beijing 100084, China

* Correspondence: wanghuaiyu@mail.tsinghua.edu.cn

Received: 11 June 2020; Accepted: 16 July 2020; Published: 17 July 2020



Abstract: The quantum phase transition of a one-dimensional transverse field Ising model in an imaginary longitudinal field is studied. A new order parameter M is introduced to describe the critical behaviors in the Yang-Lee edge singularity (YLES). The M does not diverge at the YLES point, a behavior different from other usual parameters. We term this unusual critical behavior around YLES as the pseudo-YLES. To investigate the static and driven dynamics of M , the (1+1) dimensional ferromagnetic-paramagnetic phase transition ((1+1) D FPPT) critical region, (0+1) D YLES critical region and the (1+1) D YLES critical region of the model are selected. Our numerical study shows that the (1+1) D FPPT scaling theory, the (0+1) D YLES scaling theory and (1+1) D YLES scaling theory are applicable to describe the critical behaviors of M , demonstrating that M could be a good indicator to detect the phase transition around YLES. Since M has finite value around YLES, it is expected that M could be quantitatively measured in experiments.

Keywords: Pseudo-Yang-Lee edge singularity; non-equilibrium phase transition; Kibble-Zurek scaling mechanism; non-Hermitian Ising model

1. Introduction

As one of the most interesting phenomena in many body systems, quantum phase transition occurs when parameters of a system change through a critical point, and the occurrence indicates the emergence of new physics and new states of the system [1,2]. In most of the studies of quantum phase transition, the Hamiltonians are usually assumed as Hermitian ones. Nevertheless, owing to recent experimental progress [3–9], the phase transition in non-Hermitian systems has been drawing a great deal of interest, since they can present rich behaviors different from those of Hermitian systems [10–17]. Interesting characters have been found in various non-Hermitian systems, such as the parity-time (PT) symmetry breaking phase transition induced by interface state [18,19] and the real-complex energy spectrum transition accompanied by a many-body localization-delocalization phase transition [20]. Besides these studies of equilibrium phase transition, the non-equilibrium phenomena in non-Hermitian systems have also been studied [21,22]. It was found that the Kibble-Zurek scaling (KZS) mechanism was still applicable in describing the driven dynamics across the exceptional points (EPs), where the complex spectrum becomes gapless [21].

On the other hand, Yang and Lee were the first to connect phase transitions in non-Hermitian systems with zeros of the partition function, termed Lee-Yang zeros, in the complex plane of magnetic field [23]. They showed that the zero distribution approached the positive real axis and gave the

transition point. When the applied symmetry-breaking field was imaginary, the edges of Lee-Yang zeros were singularity points in the thermodynamic limit [24]. These singularities were termed Yang-Lee edge singularities (YLES), and could be considered as a second order phase transition point with appropriate scaling laws [25–30]. The Lee-Yang zeros and YLES have been detected in recent experiments [31–33]. Theoretical investigations demonstrated that there were exotic scaling behaviors in the YLES, such as the negative correlation-length exponents, and divergence of order parameters [25]. The KZS mechanism has also been demonstrated to be applicable in the driven dynamics of YLES [34,35].

As one of the key features of YLES, the divergence of order parameter P depending on an applied field h usually exhibits as $P = |h - h_{YL}^L|^\sigma$ with $\sigma < 0$, where h_{YL}^L is the YLES point. For a one dimension (1 D) spin-1/2 Ising chain, several theoretical studies confirmed that $\sigma = -1/2$ [25,30,36–39]. By fine tuning the coupling strengths in the model, an unusual exponent of $\sigma = -3/2$ was found for a special three-state Potts model [40] and the 1 D spin-1/2 axial-next-to-nearest-neighbor model [41]. More recently, the exponent of $\sigma = -1/2$ has also been found in the scaling behaviors of the non-Hermitian Berry phase in YLES [42].

In the present research, we are going to define a new order parameter, which is not diverged at the YLES point, to character the critical behaviors around the YLES for the non-Hermitian Ising model. This order parameter obeys the similar scaling behavior with the usual order parameter but the critical exponent σ is positive. We termed this unusual scaling behavior around the YLES point as pseudo-YLES. The static behavior and the driven dynamics of this order parameter are studied in different critical regions, and KZS mechanism is still applicable to describing the behavior of this order parameter. Since the YLES points can appear at finite system size [34], the usual defined order parameter diverges at the YLES points even at small lattice size. However, the new defined order parameter is finite around the YLES points, and it is expected that this order parameter may be detected quantitatively in the experimental study.

This paper is organized as follows. In Section 2, the non-Hermitian 1 D Ising model subject to a transverse field and an imaginary longitudinal field is introduced, and the order parameter reflecting the pseudo-YLES is defined. In Section 3, the static behavior and driven dynamics of the order parameter are studied in different critical regions. A brief summary is given in Section 4.

2. The Non-Hermitian Ising Model and Order Parameter

We study a 1 D transverse-field Ising model with an imaginary longitudinal field, since this model is a typical and universal prototype to investigate the scaling behaviors in YLES [27,43,44]. The corresponding non-Hermitian Hamiltonian for a chain with length L is given by

$$H = - \sum_{n=1}^L \sigma_n^z \sigma_{n+1}^z - \lambda \sum_{n=1}^L \sigma_n^x - ih \sum_{n=1}^L \sigma_n^z, \quad (1)$$

where σ_n^x and σ_n^z are the Pauli matrices at n site in the x and z direction, respectively. The second and third terms in Equation (1) respectively present a transverse real external field and a longitudinal imaginary field. When the imaginary field is absent, the Hamiltonian becomes Hermitian.

For the Hermitian Ising model, in order to research the classical phase transition, the ordinary order parameter is usually defined as

$$\begin{aligned} M_C &= \text{Tr}(S e^{-\beta H} / \text{Tr}(e^{-\beta H})) \\ &= \text{Tr}[e^{-\beta H/2} S e^{-\beta H/2} / \text{Tr}(e^{-\beta H})], \end{aligned} \quad (2)$$

with $S = \pm 1$ and $\beta = 1/T$ being the inverse temperature. M_C is the ordinary magnetization. For the Hermitian system, M_C is real and bounded in the range of $[-1, 1]$. For the classical YLES, the order parameter can be defined in the same way of M_C , but the Hamiltonian is non-Hermitian.

Since the applied magnetic field is complex, M_C in YLES is usually complex and not bounded in the range of $[-1, 1]$. Several analytic and numerical studies have demonstrated that M_C diverges as $M_C \propto (h - h_{YL}^L)^{-1/2}$ for the model of Equation (1) [25,34,35].

For the quantum YLES, the order parameter can be defined by a quantum-classical mapping. Since the d -dimensional quantum system can be mapped to a $(d + 1)$ -dimensional classical system, the order parameter of the quantum YLES system can be defined as [27,34]

$$\begin{aligned} M_Q &= \lim_{\beta \rightarrow \infty} \text{Tr}[e^{-\beta H/2} \hat{M} e^{-\beta H/2}] / \text{Tr}(e^{-\beta H}) \\ &= \langle \psi_g^L | \hat{M} | \psi_g^R \rangle / \langle \psi_g^L | \psi_g^R \rangle, \end{aligned} \quad (3)$$

in which the operator $\hat{M} \equiv \sum_n^L \sigma_n^z / L$. $\langle \psi_g^L |$ and $|\psi_g^R \rangle$ are the normalized left and right eigenvectors satisfying $H|\psi_n^R \rangle = E_n |\psi_n^R \rangle$ and $\langle \psi_n^L | H = \langle \psi_n^L | E_n$. Moreover, the eigenvectors usually form a biorthonormal basis

$$\langle \psi_m^L | \psi_n^R \rangle = \delta_{mn}, \quad \sum_n |\psi_n^R \rangle \langle \psi_m^L | = 1. \quad (4)$$

In the non-Hermitian model, the M_Q is complex. It has been demonstrated that both the real and imaginary parts of M_Q , $M_R = \text{Re}(M_Q)$ and $M_I = \text{Im}(M_Q)$, could be used to describe critical behavior of YLES [34,35]. Around the YLES points, the static M_R and M_I scale as $M_R \propto |h - h_{YL}^L|^\sigma$ and $M_I \propto |h - h_{YL}^L|^\sigma$. For the (0+1) D YLES, $\sigma = -1/2$. Therefore, it should be difficult to quantitatively measure M_R and M_I in the experiment.

We think that it may be feasible to define some parameters that are possible to detect quantitatively experimentally. Here, we propose an order parameter evaluated in the space of the right eigenvector of the non-Hermitian system, as

$$\begin{aligned} M &= \lim_{\beta \rightarrow \infty} \text{Tr}[e^{-\beta H^+ / 2} \hat{M} e^{-\beta H / 2}] / \text{Tr}(e^{-\beta(H^+ + H)/2}) \\ &= \langle \psi_g^{R*} | \hat{M} | \psi_g^R \rangle / \langle \psi_g^{R*} | \psi_g^R \rangle, \end{aligned} \quad (5)$$

where $\langle \psi_g^{R*} |$ means the Hermitian conjugation of the right eigenvector $|\psi_g^R \rangle$. It should be noted that $\langle \psi_m^{R*} |$ and $|\psi_n^R \rangle$ are generally not orthonormal, $\langle \psi_m^{R*} | \psi_n^R \rangle \neq \delta_{mn}$. When the Hamiltonian is Hermitian, this order parameter automatically goes back to what it should be. Since the operator \hat{M} itself is Hermitian, the order parameter defined in Equation (5) is always real. Similar definition of order parameters can also be found in Refs. [20,21]. It will be shown below that M is not divergence at YLES critical points, which differs from the behaviors of usual order parameters of YLES. Recently, a method of computing mean values of observable by introducing a metric operator has been proposed [45,46], and the order parameter M can also be defined by introducing an adequate metric operator.

3. Pseudo-YLES Critical Behaviors

Before presenting our numerical results, we briefly introduce the phase structure of the model Equation (1). Since the imaginary longitudinal field has the same dimension as the real longitudinal field, Equation (1) has a ordinary ferromagnetic-paramagnetic phase transition (FPPT) point at $(g_c, h_c) = (0, 0)$ in thermal limit, where $g \equiv \lambda - \lambda_c$ and $\lambda_c = 1$ [1]. Besides this FPPT phase transition, there are also critical points for YLES at (g_{YL}^L, h_{YL}^L) for $g > 0$. The appearance of the YLES corresponds to the disappearance of energy gap between the ground state and the first excited state, which can induce critical phenomena. However, different from the FPPT, YLES can appear even at finite size, and the YLES critical points varies with system size L . Therefore, different critical regions coexist for this model: (i) around the FPPT critical point, the critical region belongs to the (1+1) D FPPT universe class; (ii) the (0+1) D YLES critical region appears near h_{YL}^L for a fixed g , and this critical region shrinks with the increase of L ; (iii) the (1+1) D YLES critical region appears near h_{YL}^∞ for a fixed g and large L ,

and h_{YL}^∞ is the critical point of the infinite-size YLES. Since the (0+1) D YLES critical region appears at finite size, different critical regions can overlap with each other. For example, at large lattice size and small g the (0+1) D YLES critical region and (1+1) D FPPT critical region overlaps with each other. On the other hand, the (0+1) D YLES critical region overlaps with the (1+1) D YLES critical region near the h_{YL}^∞ for large lattice size. In these critical regions, it was shown that KZS is still applicable, and different scaling theories could be applicable simultaneously in the overlapping region [34,35].

In present study, to investigate the pseudo-YLES critical behaviors, the static and driven dynamic behaviors of M in the (0+1) D YLES, (1+1) D FPPT and (1+1) D YLES critical regions are numerically calculated. For the sake of clarity, all usual critical exponents of the three critical regions are listed in Table 1 [1,34,35].

Table 1. Critical exponents for the (0+1) D YLES, (1+1) D FPPT and (1+1) D YLES, respectively.

(0+1) D YLES	ν_0	β_0	δ_0	z_0	r_0
	-1	1	-2	1	3
(1+1) D FPPT	ν_1	β_1	δ_1	z_1	r_1
	1	1/8	15	1	23/8
(1+1) D YLES	ν_2	β_2	δ_2	z_2	r_2
	-5/2	1	-6	1	3.4

3.1. Pseudo-YLES Critical Behaviors in the (0+1) D YLES Critical Region

Firstly, the properties of M in the (0+1) D YLES critical region is studied. It is found that at a fixed g , static M satisfies

$$M \propto |h - h_{YL}^L|^{\sigma_0}, \tag{6}$$

where $\sigma_0 > 0$ is the (0+1) D YLES critical exponent for M . The positive σ_0 is different from the divergent behaviors of usual parameters. In Figure 1, M versus $|h - h_{YL}^L|$ for different lattice size with $g = 0.01$ are plotted. In the double logarithmic coordinates, these curves are parallel straight lines. The power law fitting results show that $\sigma_0 = 0.4997 \pm 0.0005$. Furthermore, it is interesting that M is nearly the inverse of M_R around the YLES point, since $M_R \propto |h - h_{YL}^L|^{-0.5}$ [34]. Therefore, it is expected that one can experimentally measure M (M_R) by measuring M_R (M) around YLES.

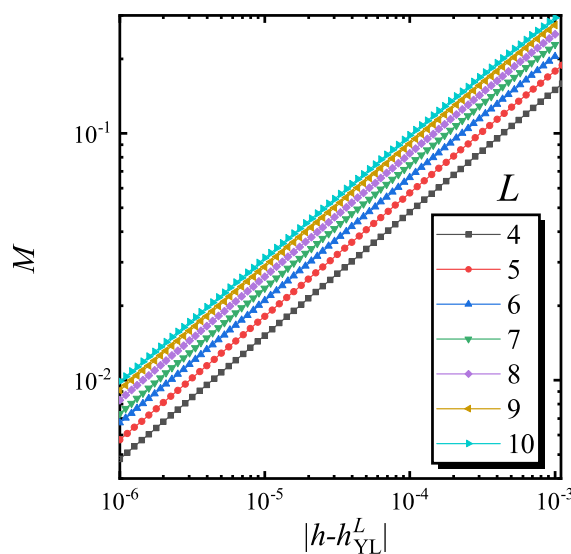


Figure 1. The curves of M versus $h - h_{YL}^L$ for different lattice size and $g = 0.01$. The power-law fitting gives that $\sigma_0 = 0.4997 \pm 0.0005$.

Next, the driven dynamics of M is studied by changing h for a fixed g . Here, we study the linear driving, namely h changes in the way of $h = h_0 + Rt$ across the critical region, since this kind of driving is widely used and readily realized in experiments. R is the varying rate of h , and it is chosen small enough and h_0 is irrelevant.

For the (0+1) D YLES critical region, it has been demonstrated that the KZS mechanism was still applicable to the driven dynamics [34]. Since the YLES can appear at finite lattice size, the driven dynamics is characterized by h and R under fixed L . The scaling function satisfies [34,47,48]

$$M(h - h_{YL}^L, R) = R^{s_0} f_1[(h - h_{YL}^L)R^{\frac{\beta_0 \delta_0}{\nu_0 r_0}}]. \quad (7)$$

In Equation (7), s_0 is the scaling factor of M for the driven dynamics, and $r_0 = z_0 + \beta_0 \delta_0 / \nu_0$ with z_0 , β_0 and ν_0 being the usual critical exponents for the (0+1) D YLES as shown in Table 1 [25,34], and f_1 is the scaling function of the (0+1) D YLES driven dynamics. It should be noted that the lattice size is not involved in this scaling function. At h_{YL}^L , $M_{YL}^L = M(h_{YL}^L - h_{YL}^L, R) \propto R^{s_0}$. Therefore, by fitting the curve of M_{YL}^L versus R , s_0 can be determined.

To verify the scaling function Equation (7), we numerically solved Schrödinger equation for model Equation (1) under periodic boundary condition. The finite difference method in the time direction is used, and the time interval is chosen as 2×10^{-5} in our calculation. Initial condition being $h = h_0$, the exact diagonalization is carried out. The lowest real eigenenergy is obtained and the corresponding right eigenstate is set as the initial state. Since the Hamiltonian is non-Hermitian, the wave function is normalized as $\langle \Psi_R^* | \Psi_R \rangle = 1$ after each step of evolution.

In Figure 2, M_{YL}^L versus R for $L = 4$ to 10 are plotted. These lattice sizes correspond to the small and middle size systems. The curves are parallel straight lines in the double logarithmic coordinates, indicating that the scaling function Equation (7) and s_0 are universal for different size. By a power law fitting, it is found that $s_0 = 0.3348 \pm 0.0007$. Since the driven dynamics of M_R shows that $M_R[(h_{YL}^L - h_{YL}^L), R] \propto R^{\beta_0 / \nu_0 r_0} = R^{-1/3}$ [34], M_{YL}^L is also nearly the inverse of $M_R[(h_{YL}^L - h_{YL}^L), R]$. We select $L = 10$ and calculate the driven dynamics with a fixed g to verify the scaling function of Equation (7). In Figure 3, M versus h for different R and the rescaled curves are plotted. The rescaled curves collapse onto each other, indicating that the driven dynamics can be well described by scaling function Equation (7).

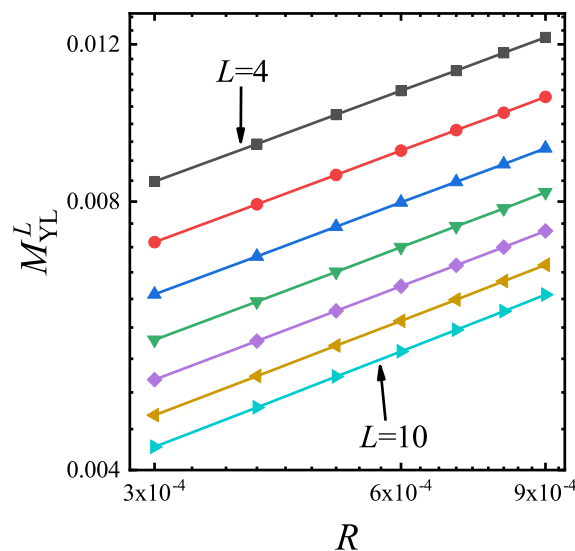


Figure 2. The curves of M_{YL}^L versus R for different lattice size and $g = 3$ in the double logarithmic coordinates. Power law fitting gives that $s_0 = 0.3348 \pm 0.0007$. From top to bottom, the lattice size is 4 to 10.

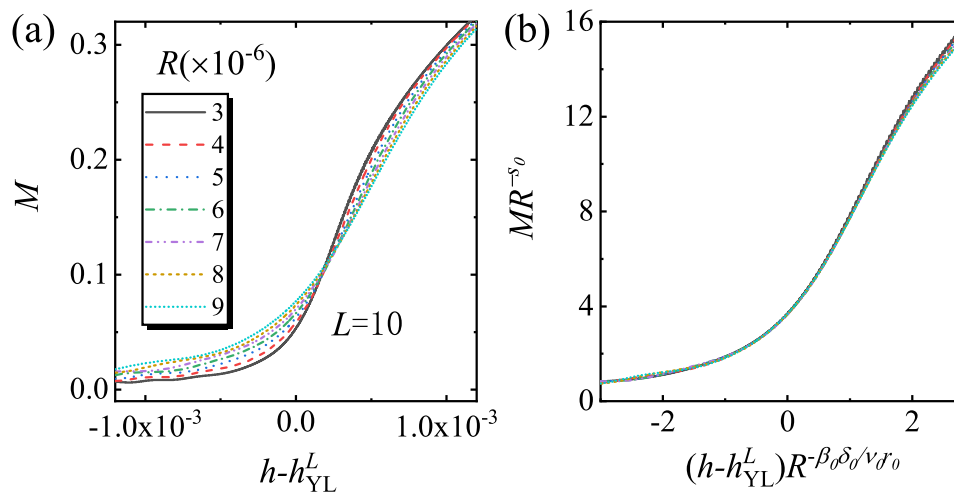


Figure 3. (a) The curves of M versus $h - h_{YL}^L$ for different R with $L = 10$ and (b) the rescaled curves of MR^{-s_0} versus $(h - h_{YL}^L)R^{-\beta_0\delta_0/\nu_0}$ according to Equation (7). Here, $g = 0.001$ and $h_{YL}^L = 0.010558$.

3.2. Critical Behaviors of M in the (1+1) D FPPT and (1+1) D YLES Critical Region

In this subsection, the critical behaviors of M in the critical regions of (1+1) D FPPT and (1+1) D YLES is studied.

For the (1+1) D FPPT critical region, the order parameter M should satisfy a similar scaling form in the real longitudinal-field case. The static M satisfies the following relation [35,47].

$$M = L^{-\beta_1/\nu_1} f_2(gL^{1/\nu_1}, hL^{\beta_1\delta_1/\nu_1}). \tag{8}$$

Here, f_2 is the scaling function for M , and β_1, δ_1 and ν_1 are the 2 D classical FPPT critical exponents as shown in Table 1 [1]. These parameters are used to describe the scaling behaviors of quantum Ising chains.

To confirm the relation in Equation (8), the static M versus h was calculated with a fixed gL^{1/ν_1} . Here, we choose that g is small and L is large, so that the system is in the (1+1) D FPPT critical region. In Figure 4a, M versus h with different lattice size is plotted. In these curves, the knee points correspond to YLES points h_{YL}^L . After rescaling according to Equation (8), the rescaled curves of ML^{β_1/ν_1} versus $hL^{\beta_1\delta_1/\nu_1}$ match with each other as shown in Figure 4b.

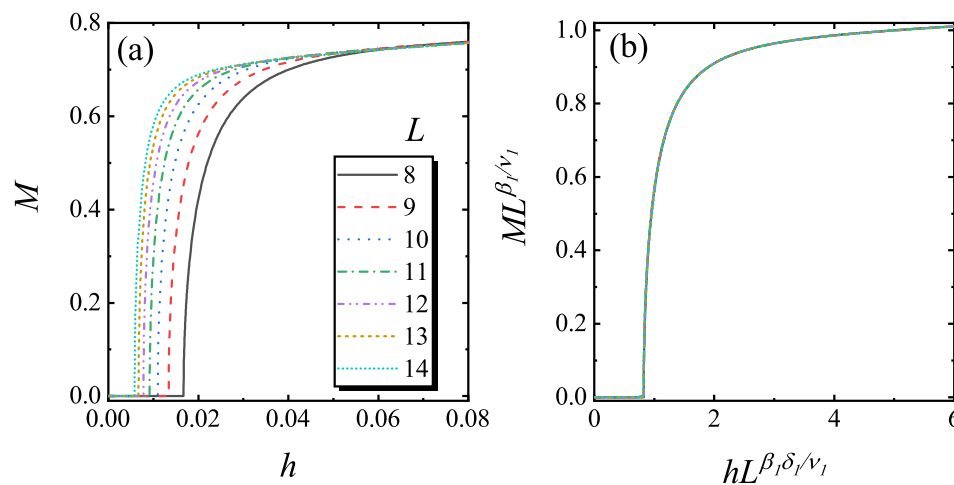


Figure 4. The curves of static M versus h for different L for fixed $gL^{1/\nu_1} = 0.06$ (a) and the rescaled curves of ML^{β_1/ν_1} versus $hL^{\beta_1\delta_1/\nu_1}$ (b) according to Equation (8).

The driven dynamics in the (1+1) D FPPT critical region is characterized by h , R and L . The scaling form of M reads [35]

$$M(g, h, L, R) = R^{\frac{\beta_1}{\nu_1 r_1}} f_3(gR^{-\frac{1}{\nu_1 r_1}}, L^{-1}R^{-\frac{1}{r_1}}, hR^{-\frac{\beta_1 \delta_1}{\nu_1 r_1}}), \tag{9}$$

where r_1 and z_1 are the critical exponent of the (1+1) D FPPT and f_3 is a scaling function. By fixing $gR^{-\frac{1}{\nu_1 r_1}}$ and $L^{-1}R^{-\frac{1}{r_1}}$ in Equation (9), the curves of M as a function of h for different lattice size are calculated. The results are plotted in Figure 5a. The rescaled curves of $MR^{-\frac{\beta_1}{\nu_1 r_1}}$ versus $hR^{-\frac{\beta_1 \delta_1}{\nu_1 r_1}}$ match with each other very well as shown in Figure 5b, which confirms the scaling function of Equation (9). Moreover, from Figure 5a, M for different L reach a saturation value at large h but still less than 1, which means M is bounded in the range of $[-1,1]$ as the order parameter defined in the Hermitian system.

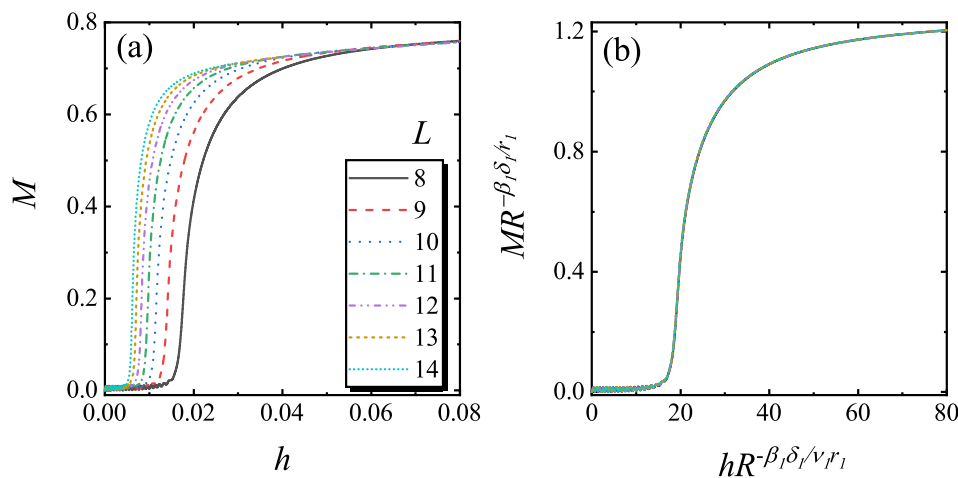


Figure 5. (a) The curves of M versus h for different L with $gR^{-\frac{1}{\nu r}} = 0.3133$ and $L^{-1}R^{\frac{1}{r}} = 0.1915$ and (b) the rescaled curves of $MR^{-\beta\delta/r}$ versus $hR^{-\beta\delta/vr}$ according to Equation (9).

Near h_{YL}^∞ for a fixed g , the scaling dynamics of M of the medium lattice size should satisfy the (1+1) D KZS with the finite-size corrections being considered. Following the (1+1) D YLES scaling theory, the scaling form of M reads [34]

$$M(h - h_{YL}^\infty, R, L) = R^{s_2} f_4 \left[(h - h_{YL}^\infty)R^{-\frac{\beta_2 \delta_2}{\nu_2 r_2}}, L^{-1}R^{-1/r_2} \right], \tag{10}$$

where β_2 , δ_2 , ν_2 and r_2 are the critical exponents of the (1+1) D YLES critical theory (see Table 1) [34], and s_2 is the (1+1) D YLES critical exponent for M . By fixing $L^{-1}R^{-1/r_2}$ in Equation (10), s_2 can be obtained by fitting $M_{YL}^\infty = M(h_{YL}^\infty - h_{YL}^\infty, R, L)$ verse R .

To verify the scaling function of Equation (10), s_2 is firstly determined by fitting M_{YL}^∞ versus R for a fixed $L^{-1}R^{-1/r_2}$. Here, g is chosen as $g = 4$, which is large enough to ensure that the system is not in the critical region of (1+1) D YLES. In Figure 6, M_{YL}^∞ versus R and the fitted curve are plotted, and it is achieved that $s_2 = 0.5816$. In Figure 7, M verses h and the rescaled curves according to Equation (10) are plotted. We find that the rescaled curve matches with each other, confirming Equation (10).

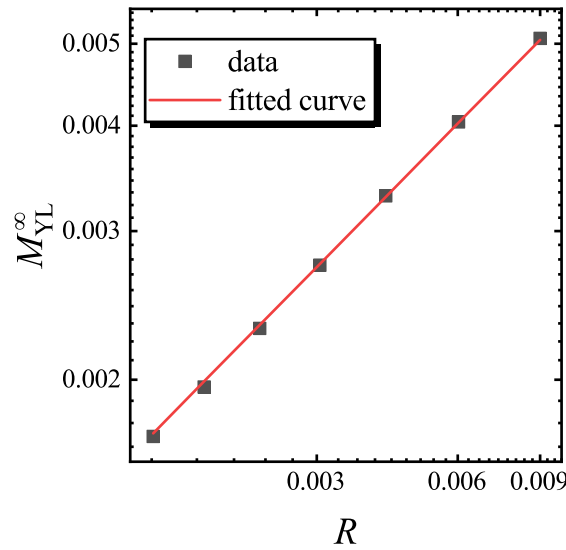


Figure 6. The curve of M_{YL}^∞ versus R and the fitted curve with fixed $L^{-1}R^{-1/r_2} = 2.001689$ in the double logarithmic coordinates. The fitting curve is $M_{YL}^\infty \propto R^{0.5816}$. Here, $h_{YL}^\infty = 2.292425$ and $g = 4$.

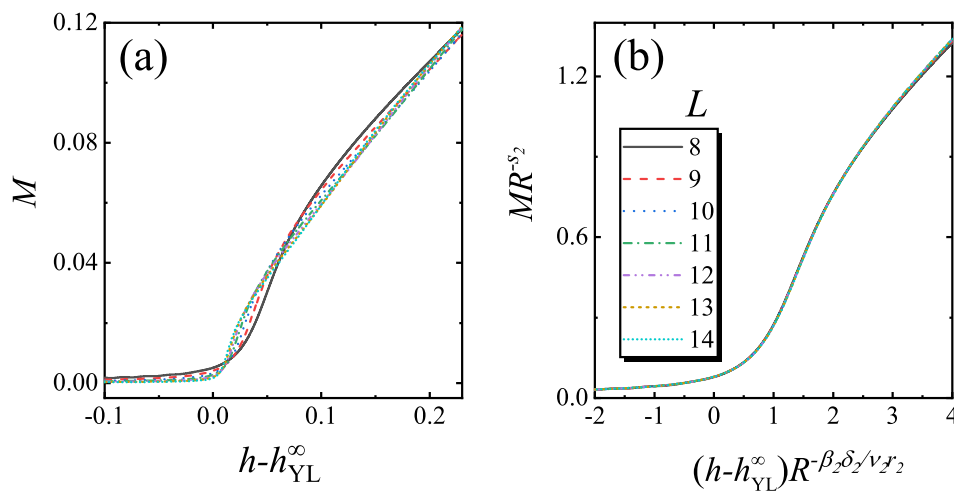


Figure 7. (a) The curves of M versus h for different L with $L^{-1}R^{-1/r_2} = 2.001689$ and (b) the rescaled curves of MR^{-s_2} versus $(h - h_{YL}^\infty)R^{-\beta_2\delta_2/\nu_2r_2}$ according to Equation (10). Here, $h_{YL}^\infty = 2.292425$ and $g = 4$.

Finally, we have some discussion with respect to the defined M . Suppose that the wave functions have been normalized, $\langle \psi_n^L | \psi_n^R \rangle = 1$. Then

$$M_Q = \frac{1}{\langle \psi_g^{R*} | \psi_g^R \rangle} \langle \psi_g^{R*} | \psi_g^R \rangle \langle \psi_g^L | \hat{M} | \psi_g^R \rangle. \tag{11}$$

Now we use the complete set Equation (4), so as to get $|\psi_g^R\rangle\langle\psi_g^L| = 1 - \sum_{n \neq g} |\psi_n^R\rangle\langle\psi_n^L|$. One immediately find that

$$M_Q = M - \frac{1}{\langle \psi_g^{R*} | \psi_g^R \rangle} \langle \psi_g^{R*} | \sum_{n \neq g} |\psi_n^R\rangle\langle\psi_n^L| \hat{M} | \psi_g^R \rangle, \tag{12}$$

which means that the behavior of M_Q includes M and the information of the highly excited states. Moreover, We have confirmed numerically that the static behavior of the second term in Equation (12) have similar scaling behaviors but opposite with M_Q around the YLES points. Therefore, the divergence

of M_Q and the second term in Equation (12) can result in a non-divergence behavior of M . From this equation it is understood that the divergence is from the contribution of excited states. The ground state itself does not yield divergence. The behavior of M_Q reflects the effect from all possible excited states, while the definition of M seems get rid of the influence from excited states. Therefore, the definition of M is really a good way to present an index which is finite at critical point.

4. Summary

In summary, the pseudo-YLES critical behavior has been studied in this paper. An order parameter has been suggested to study the static properties and driven dynamics of pseudo-YLES. We have found that M scales as $M \propto |h - h_{YL}^L|^{\sigma_0}$ around the YLES points, with positive σ_0 that is different from the usual order parameters, and M is not divergence at the YLES points. The static and driven dynamics of M are studied in the (0+1) D YLES, (1+1) D FPPT and (1+1) D YLES critical regions, and it is found that the scaling behaviors can be described by the (0+1) D YLES, (1+1) D FPPT and (1+1) D YLES scaling theories, respectively. These results demonstrate that M could be a good indicator of phase transition in YLES. Moreover, since the static M is finite around the YLES points, it is expected that M may be easier to measure experimentally rather than the usual order parameters. Although not shown here, the order parameter can also be defined in the left eigenvector space, and the order parameter in the left eigenvector space also satisfies the conclusions obtained above.

Author Contributions: Conceptualization, H.-Y.W. and G.-Y.H.; methodology, G.-Y.H. and L.-J.Z.; software, L.-J.Z.; formal analysis, G.-Y.H.; investigation, L.-J.Z., H.-Y.W. and G.-Y.H.; writing—original draft preparation, L.-J.Z. All authors have read and agreed to the published version of the manuscript.

Funding: This research was funded by the Natural Science Foundation of Jiangsu Province (Grant No. BK20170309) and National Natural Science Foundation of China (Grant No. 11704161 and 11547142).

Conflicts of Interest: The authors declare no conflict of interest.

Abbreviations

The following abbreviations are used in this manuscript:

YLES	Yang-Lee edge singularity
EP	exceptional point
FPPT	ferromagnetic-paramagnetic phase transition
KZS	Kibble-Zurek scaling

References

1. Sachdev, S. *Quantum Phase Transitions*; Cambridge University Press: Cambridge, UK, 2011.
2. Dziarmaga, J. Dynamics of a quantum phase transition and relaxation to a steady state. *Adv. Phys.* **2010**, *59*, 1063–1189. [[CrossRef](#)]
3. Klinder, J.; Kessler, H.; Wolke, M.; Mathey, L.; Hemmerich, A. Dynamical phase transition in the open Dicke model. *Proc. Natl. Acad. Sci. USA* **2015**, *112*, 3290–3295. [[CrossRef](#)] [[PubMed](#)]
4. El-Ganainy, R.; Makris, K.G.; Khajavikhan, M.; Musslimani, Z.H.; Rotter, S.; Christodoulides, D.N. Non-Hermitian physics and PT symmetry. *Nat. Phys.* **2018**, *14*, 11–19. [[CrossRef](#)]
5. Zeuner, J.M.; Rechtsman, M.C.; Plotnik, Y.; Lumer, Y.; Nolte, S.; Rudner, M.S.; Segev, M.; Szameit, A. Observation of a Topological Transition in the Bulk of a Non-Hermitian System. *Phys. Rev. Lett.* **2015**, *115*, 040402. [[CrossRef](#)] [[PubMed](#)]
6. Rüter, C.E.; Makris, K.G.; El-Ganainy, R.; Christodoulides, D.N.; Segev, M.; Kip, D. Observation of parity-time symmetry in optics. *Nat. Phys.* **2010**, *6*, 192–195. [[CrossRef](#)]
7. Zhang, X.; Ding, K.; Zhou, X.; Xu, J.; Jin, D. Experimental Observation of an Exceptional Surface in Synthetic Dimensions with Magnon Polaritons. *Phys. Rev. Lett.* **2019**, *123*, 237202. [[CrossRef](#)]
8. Xu, H.; Mason, D.; Jiang, L.; Harris, J.G.E. Topological energy transfer in an optomechanical system with exceptional points. *Nature* **2016**, *537*, 80–83. [[CrossRef](#)]

9. Barontini, G.; Labouvie, R.; Stubenrauch, F.; Vogler, A.; Guarrera, V.; Ott, H. Controlling the Dynamics of an Open Many-Body Quantum System with Localized Dissipation. *Phys. Rev. Lett.* **2013**, *110*, 035302. [[CrossRef](#)]
10. Moiseyev, N. *Non-Hermitian Quantum Mechanics*; Cambridge University Press: Cambridge, UK, 2011.
11. Longhi, S. Topological Phase Transition in non-Hermitian Quasicrystals. *Phys. Rev. Lett.* **2019**, *122*, 237601. [[CrossRef](#)]
12. Wei, B.-B.; Jin, L. Universal Critical Behaviours in Non-Hermitian Phase Transitions. *Sci. Rep.* **2017**, *7*, 7165. [[CrossRef](#)]
13. Lee, T.E.; Reiter, F.; Moiseyev, N. Entanglement and Spin Squeezing in Non-Hermitian Phase Transitions. *Phys. Rev. Lett.* **2014**, *113*, 250401. [[CrossRef](#)]
14. Ni, X.; Smirnova, D.; Poddubny, A.; Leykam, D.; Chong, Y.; Khanikaev, A.B. \mathcal{PT} phase transitions of edge states at \mathcal{PT} symmetric interfaces in non-Hermitian topological insulators. *Phys. Rev. B* **2018**, *98*, 165129. [[CrossRef](#)]
15. Bender, C.M. Making sense of non-Hermitian Hamiltonians. *Rep. Prog. Phys.* **2007**, *70*, 947. [[CrossRef](#)]
16. Zhou, L.; Wang, Q.-H.; Wang, H.; Gong, J. Dynamical quantum phase transitions in non-Hermitian lattices. *Phys. Rev. A* **2018**, *98*, 022129. [[CrossRef](#)]
17. Kawabata, K.; Shiozaki, K.; Ueda, M.; Sato, M. Symmetry and Topology in Non-Hermitian Physics. *Phys. Rev. X* **2019**, *9*, 041015. [[CrossRef](#)]
18. Schomerus, H. Topologically protected midgap states in complex photonic lattices. *Opt. Lett.* **2013**, *38*, 1912–1914. [[CrossRef](#)]
19. Zhao, H.; Longhi, S.; Feng, L. Robust Light State by Quantum Phase Transition in Non-Hermitian Optical Materials. *Sci. Rep.* **2015**, *5*, 17022. [[CrossRef](#)]
20. Hamazaki, R.; Kawabata, K.; Ueda, M. Non-Hermitian Many-Body Localization. *Phys. Rev. Lett.* **2019**, *123*, 090603. [[CrossRef](#)]
21. Dora, B.; Heyl, M.; Moessner, R. The Kibble-Zurek mechanism at exceptional points. *Nat. Commun.* **2019**, *10*, 2254. [[CrossRef](#)]
22. Xue, P.; Xiao, L.; Qu, D.; Wang, K.; Li, H.-W.; Dai, J.-Y.; Dora, B.; Heyl, M.; Moessner, R.; Yi, W. Non-Hermitian Kibble-Zurek mechanism with tunable complexity in single-photon interferometry. *arXiv* **2020**, arXiv:2004.05928. [[CrossRef](#)]
23. Yang, C.N.; Lee, T.D. Statistical Theory of Equations of State and Phase Transitions. I. Theory of Condensation. *Phys. Rev.* **1952**, *87*, 404–409.
24. Lee, T.D.; Yang, C.N. Statistical Theory of Equations of State and Phase Transitions. II. Lattice Gas and Ising Model. *Phys. Rev.* **1952**, *87*, 410–419. [[CrossRef](#)]
25. Fisher, M.E. Yang-Lee Edge Singularity and ϕ^3 Field Theory. *Phys. Rev. Lett.* **1978**, *40*, 1610–1613. [[CrossRef](#)]
26. Bessis, J.D.; Drouffe, J.M.; Moussa, P. Positivity constraints for the Ising ferromagnetic model. *J. Phys. A Math. Gen.* **1976**, *9*, 2105–2124. [[CrossRef](#)]
27. Uzelac, K.; Pfeuty, P.; Jullien, R. Yang-Lee Edge Singularity from a Real-Space Renormalization-Group Method. *Phys. Rev. Lett.* **1979**, *43*, 805–808. [[CrossRef](#)]
28. Kurtze, D.A.; Fisher, M.E. Yang-Lee edge singularities at high temperatures. *Phys. Rev. B* **1979**, *20*, 2785–2796. [[CrossRef](#)]
29. Wang, X.-Z.; Kim, J.S. The Critical Line of an Ising Antiferromagnet on Square and Honeycomb Lattices. *Phys. Rev. Lett.* **1997**, *78*, 413–416. [[CrossRef](#)]
30. Wang, X.-Z.; Kim, J.S. Yang-Lee edge singularity of a one-dimensional Ising ferromagnet with arbitrary spin. *Phys. Rev. E* **1998**, *58*, 4174–4180. [[CrossRef](#)]
31. Peng, X.; Zhou, H.; Wei, B.-B.; Cui, J.; Du, J.; Liu, R.-B. Experimental Observation of Lee-Yang Zeros. *Phys. Rev. Lett.* **2015**, *114*, 010601. [[CrossRef](#)]
32. Brandner, K.; Maisi, V.F.; Pekola, J.P.; Garrahan, J.P.; Flindt, C. Experimental Determination of Dynamical Lee-Yang Zeros. *Phys. Rev. Lett.* **2017**, *118*, 180601. [[CrossRef](#)]
33. Wei, B.-B. Probing Yang-Lee edge singularity by central spin decoherence. *New J. Phys.* **2017**, *19*, 083009. [[CrossRef](#)]
34. Yin, S.; Huang, G.-Y.; Lo, C.-Y.; Chen, P. Kibble-Zurek Scaling in the Yang-Lee Edge Singularity. *Phys. Rev. Lett.* **2017**, *118*, 065701. [[CrossRef](#)]

35. Zhai, L.-J.; Wang, H.-Y.; Yin, S. Hybridized Kibble-Zurek scaling in the driven critical dynamics across an overlapping critical region. *Phys. Rev. B* **2018**, *97*, 134108. [[CrossRef](#)] [[PubMed](#)]
36. Kortman, P.; Griffiths, R. Density of Zeros on the Lee-Yang Circle for Two Ising Ferromagnets. *Phys. Rev. Lett.* **1971**, *27*, 1439–1442. [[CrossRef](#)]
37. Fisher, M.E. Yang-Lee Edge Behavior in One-Dimensional Systems. *Supp. Prog. Theor. Phys.* **1980**, *69*, 14–29. [[CrossRef](#)]
38. Glumac, Z.; Uzelac, K. The partition function zeros in the one-dimensional q-state Potts model. *J. Phys. A Math. Gen.* **1994**, *27*, 7709–7717. [[CrossRef](#)]
39. Ghulghazaryan, R.G.; Sargsyan, K.G.; Ananikian, N.S. Partition function zeros of the one-dimensional Blume-Capel model in transfer matrix formalism. *Phys. Rev. E* **2007**, *76*, 021104. [[CrossRef](#)]
40. Mittag, L.; Stephen, M.J. Yang-Lee Zeros of the Potts Model. *J. Stat. Phys.* **1984**, *35*, 303. [[CrossRef](#)]
41. Dalmazi, D.; Sá, F.L. Unusual Yang-Lee edge singularity in the one-dimensional axial-next-to-nearest-neighbor Ising model. *Phys. Rev. E* **2010**, *82*, 051108. [[CrossRef](#)]
42. Zhai, L.-J.; Wang, H.-Y.; Huang, G.-Y. Scaling of the Berry Phase in the Yang-Lee Edge Singularity. *Entropy* **2019**, *21*, 836. [[CrossRef](#)]
43. Castro-Alvaredo, O.A.; Fring, A. A spin chain model with non-Hermitian interaction: The Ising quantum spin chain in an imaginary field. *J. Phys. A Math. Theor.* **2009**, *42*, 465211. [[CrossRef](#)]
44. Von Gehlen, G. Critical and off-critical conformal analysis of the Ising quantum chain in an imaginary field. *J. Phys. A Math. Gen.* **1991**, *24*, 5371. [[CrossRef](#)]
45. Ramírez, R.; Reboiro, M. Dynamics of finite dimensional non-hermitian systems with indefinite metric. *J. Math. Phys.* **2019**, *60*, 012106. [[CrossRef](#)]
46. Jean-Pierre Antoine, J.-P.; Trapani, C. Operator (Quasi-)Similarity, Quasi-Hermitian Operators and All that. In *Non-Hermitian Hamiltonians in Quantum Physics*; Bagarello, F., Passante, R., Trapani, C., Eds.; Springer: Berlin, Germany, 2015; p. 45. [[CrossRef](#)]
47. Gong, S.; Zhong, F.; Huang, X.; Fan, S. Finite-time scaling via linear driving. *New J. Phys.* **2010**, *12*, 043036.
48. Chandran, A.; Erez, A.; Gubser, S.S.; Sondhi, S.L. Kibble-Zurek problem: Universality and the scaling limit. *Phys. Rev. B* **2012**, *86*, 064304. [[CrossRef](#)]



© 2020 by the authors. Licensee MDPI, Basel, Switzerland. This article is an open access article distributed under the terms and conditions of the Creative Commons Attribution (CC BY) license (<http://creativecommons.org/licenses/by/4.0/>).